Taylor & Francis
Taylor & Francis Group

Inhalation Toxicology

International Forum for Respiratory Research

ISSN: 0895-8378 (Print) 1091-7691 (Online) Journal homepage: http://www.tandfonline.com/loi/iiht20

Fiber Deposition in the Tracheobronchial Region: Deposition Equations

Yue Zhou, Wei-Chung Su & Yung Sung Cheng

Inhalation Toxicology, 20:1191–1198, 2008

ISSN: 0895-8378 print / 1091-7691 online
DOI: 10.1080/08958370802233082

informa
healthcare

Fiber Deposition in the Tracheobronchial Region: Deposition Equations

Yue Zhou, Wei-Chung Su, and Yung Sung Cheng
Lovelace Respiratory Research Institute, Albuquerque, New Mexico, USA

A lung deposition model for fibrous aerosol needs accurate deposition equations for different regions of the human respiratory tract. For fiber deposition in the tracheobronchial region there are several theoretical and empirical equations to predict deposition efficiency in the impaction-dominant region. However, few were verified with experimental data. We have obtained experimental data of fiber deposition in realistic human airway replicas using carbon fibers. Comparison of experimental data and existing deposition models yield variable results, with some models performing better than other models. There was no consistent agreement found over the Stokes number range of experimental data. A generic empirical model for fiber deposition in the tracheobronchial region was developed based on all carbon fiber deposition data in human lung replicas. This model includes the size of fibers and the geometry of the tracheobronchial bifurcation. Because it is difficult to develop only one equation for all data from the trachea to the major bronchial bifurcations, the deposition patterns in the trachea and first generation were each predicted by their own equations. An additional equation was developed for the second to fourth generations. This model, combined with oral and nasal deposition predictions which will be published elsewhere, can be used to investigate the inhalation dosimetry and deposition patterns of fibers in human lungs for assessing occupational hazards and air pollutants.

INTRODUCTION

Fibrous particles are those with an elongated shape. They are widely used in various industrial fields due to their low cost and highly desirable physical/chemical properties, such as high heat resistance. However, fibers have also been associated with potential health hazards when they are inhaled and deposited in the lungs. Four major deposition mechanisms: impaction, interception, sedimentation, and diffusion, contribute to fiber deposition in the lungs depending on the fiber's dimensions, the inspiration flow rate, and the lungs' geometry. In general, deposition occurs with a combination of these mechanisms.

Theoretical prediction of fiber deposition in the lungs began in the 1970s when Beeckmans (1970) used Weibel's lung model (1963) to calculate the deposition of asbestos by treating the fibers as randomly oriented prolate spheroids. By neglecting interception, Beeckmans' results showed that deposition decreased with the increase of the fiber length for fibers having a constant diameter. Two years later, Harris (1972) developed a fiber deposition model using the Task Group on Lung Dynamics model (1966) together with Weibel's anatomical model. Fibers were again treated as stretch spheroids and the four deposition mechanisms were expressed separately according to fiber size and dynamic conditions. The deposition equations for impaction, diffusion, and sedimentation were modified from those derived from spherical particles and interception of fibers was included as well. Asgharian & Yu (1988) considered fiber rotation in their deposition equations in their human lung deposition model. Total deposition of fibers in the lung using mouth breathing was found to be smaller than that of spherical fibers with the same mass. Recently, Sturm & Hofmann (2006) proposed a fiber deposition simulation computer model termed FIBROS, where the input window included selection of the breathing condition, the fiber's physical properties, as well as the deposition equations for the tracheobronchial airways. Their simulation indicated that using different deposition equations results in substantial variation in regional deposition. There were no human experimental data for fiber deposition; therefore, these models remained to be verified.

An asymmetrical multiple-path model of fiber deposition in rats was also developed by Asgharian & Anjilvel (1998). Their calculations on total deposition were in agreement with experimental data reported in the literature (Evans et al., 1973; Morgan

Received 23 April 2008; accepted 28 May 2008.
The authors are grateful to W.T. Fan for technical assistance, and Vick Fisher for reviewing this manuscript. This project is sponsored by NIOSH grant R01 OH003900.
Address correspondence to Yue Zhou, 2425 Ridgecrest Drive SE, Albuquerque, NM 87108, USA. E-mail: yzhou@lrri.org

et al., 1978; Griffis et al., 1981; Roggli & Brody, 1984). Ding et al. (1997) proposed a nasal deposition equation for rats based on experimental results obtained from spherical particles in rats' nasal passages. They used this equation in the rat lung deposition model and made extensive comparisons with experimental data. The model prediction for total and nasal deposition was in general agreement with the experimental data, but in several cases the prediction was higher than the experimental data. The model calculation for pulmonary deposition agreed well with the experimental data.

Several deposition equations have been developed and used for calculating tracheobronchial deposition in the human deposition models. According to fiber movement in the tracheobronchial tree, Cai & Yu (1988) proposed a deposition model assuming a simple flow field in the airway bifurcations. Only inertial impaction and interception mechanisms were considered in the model. With the development of computer technology, many theoretical models for fiber deposition in human lungs were achieved by computational fluid dynamics (CFD) techniques (Balásházy et al., 2005; Zhang et al., 1996; Podgorski et al., 1995; Asgharian & Anjilvel, 1995). These numerical models are very complicated and not easy to use without the computer code. Empirical equations developed from experimental data obtained in physical airway replicas (Sussman et al., 1991a,1991b; Myojo & Takaya, 2001) have also been considered in the lung model.

The major issue with these fiber deposition models, especially in human models, is the verification with the experimental data. Due to the lack of information on *in vivo* fiber deposition in human volunteers, experimental results obtained in realistic airway replicas would be useful. Experimental studies conducting fiber deposition in realistic human replicas, including nasal, oral, and tracheobronchial deposition, have been reported (Su & Cheng, 2005, 2006a, 2006b; Zhou et al., 2007). In this paper we report extensive comparison of deposition equations with experimental data on fiber obtained from tracheobronchial regions in several airway replicas (Sussman et al., 1991a; Zhou et al., 2007). Based on this study, we made several recommendations on modeling fiber deposition in humans.

MATERIALS AND METHODS

Experimental Methods

A description of experimental design and methods for the deposition of fibers in human airway replica has been reported (Zhou et al., 2007). Briefly, two different human lung replicas, casts A and B, which included the oral cavity, pharynx, larynx, trachea, and three to four generations of bronchi along with conductive carbon fibers (Hercules Inc., Wilmington, DE) having a monodisperse diameter of 3.66 μm and polydisperse in length (Su & Cheng, 2005) were used in this study. Fibrous particles generated from a small-scale powder disperser (Model 3433; TSI Inc., St. Paul, MN) were led to an aerosol Kr-85 neutralizer in a chamber where they were neutralized and well mixed with the diluted air. To avoid particle re-bounce, the inner surface of the replicas was coated with silicon oil. Fibers were then passed through the lung replica at three inspiratory flow rates of 15, 43.5, and 60 L/min, which cover the breathing rate of a human adult from rest to moderate exercise. For each replica, each terminal tube of the replica was connected to a 25-mm asbestos filter cassette to collect fibers that passed through the replica. After each aerosol exposure the replica was cut into segments and washed with alcohol. The alcohol solution was then filtered to obtain the sample slides. Each slide was analyzed with a microscope to determine the fiber length distribution and number concentration. The deposition efficiency of a bifurcation for fiber of a certain length was calculated by the number of fibers deposited in the bifurcation divided by total fibers before entering the bifurcation. The deposition efficiency of each bifurcation as a function of fiber dimension and flow rate was then calculated.

Deposition Equations

Three theoretical and two empirical models developed for fiber deposition in the tracheobronchial region were used in the lung deposition models. Most of these fiber deposition models were based on inertial deposition region, and impaction was considered the major mechanism in those models. These models can be used to estimate the regional deposition and dose for inhaled fibers. Except for the empirical model of Sussman et al. (1991b), which used a realistic human lung cast as a physical model, those models were all based on the idealized, symmetrical airway bifurcations. The method developed by Cai & Yu (1988) only considered the impaction and interception mechanisms based on the concept of the stop and interception distances of a particle in the cross-section of the daughter tube. The fiber deposition model was a modification of the spherical particle deposition model. For uniform flow, three different fiber orientations were considered, 1) parallel to the axis of the daughter tube, 2) parallel to the parent tube and remains so at the bifurcation, and 3) random orientation. The first case represents strong fiber alignment by the primary flow, so that the effect of the interception can be ignored. The deposition efficiency (η) is only based on the impaction as follows:

$$\eta = F\left(\alpha, \frac{R}{R_0}\right) Stk_1 \qquad [1]$$

where F (Cai & Yu, 1988) is the function of bifurcation angle (α) and the ratio of radius for daughter (R) and parent (R_0). The Stk_1 is the Stokes number for this specific case. Because cases 2 and 3 include interception as another deposition mechanism, the deposition efficiencies can be expressed by:

$$\eta = F\left(\alpha, \frac{R}{R_0}\right) Stk_i + H_i(\alpha)\frac{l_f}{R} \qquad [2]$$

where i is 2 or 3 representing either case 2 or 3, H (Cai & Yu, 1988) is a function of the bifurcation angle having different expressions in different cases, and l_f is the fiber length.

Zhang and co-workers (1996) made numerical simulations on flow field and fiber trajectory with orientations in a three-dimensional bifurcation airway. The bifurcation had the same diameter of 0.6 cm for both parent and daughter tubes. A computer code was developed to calculate fiber transport in the airway tubes using the equations for fiber motions. The deposition efficiency was obtained with different bifurcation angles and Reynolds numbers as a function Stokes number. A similar calculation was made by Balásházy et al. (2005) with a stochastic lung deposition model for different flow rates and equivalent diameters. Deposition efficiencies for mouth or nasal breathing were also calculated in their study. Results showed the deposition efficiency as a function of lung generations or fiber length.

Two brass bifurcations, which corresponded to the second to fourth generations of Weibel's lung model, were used by Myojo (1987, 1990) for the fiber deposition experiment. After delivering fibers to the bifurcation models, fibers were counted under a scanning electron microscope. Based on more experimental data, Myojo & Takaya (2001) introduced an empirical model for fiber deposition in a bifurcation and considered the interception parameter and Stokes number in their model. This model gave five constant parameters based on the experimental data.

An empirical model that predicts fiber deposition in the human tracheobronchial region was developed by Sussman et al. (1991a,1991b). Based on the experimental data of asbestos deposited in a realistic human airway replica, a "best fit" equation for all fibers' deposition efficiency (η) was introduced as:

$$\eta = 0.052 + 0.007\log(\rho d^2 Q) + 3.54 D_{\text{int}} \qquad [3]$$

where ρ is the fiber density, d is the fiber equivalent aerodynamic diameter, Q is the inhalation flow rate, and D_{int} is a function of fiber length and radius of a parent generation.

Calculation of Stokes Number

The Stokes number is a dimensionless parameter that includes particle size, velocity, and lung geometry. It is easier to compare particle deposition results from different lung geometry and inhalation patterns by using the Stokes number. For a spherical particle traveling in a tube, the Stokes number is simply a function of particle diameter, travel velocity, and the diameter of the tube. However, the Stokes number of a fiber also includes the fiber orientation in the flow. The calculation of the Stokes number for a fiber varies in different theoretical models. The model of Cai & Yu (1988) used the equivalent diameters of a fiber for Stokes drag introduced by Oseen (1927) in the Stokes calculation. For a fiber randomly orientated in the stream, the Stokes number (*Stk*) used by Cai & Yu (1988) can be expressed as

$$Stk = \frac{\rho d_f^3 \beta U_0}{36\mu\left((1-\frac{\pi^2}{16})d_{f//} + \frac{\pi^2}{16} d_{f\perp}\right) R_0} \qquad [4]$$

where ρ is the fiber density, d_f is the fiber diameter, β is the aspect ratio, U_0 is the velocity of the flow, and μ is air viscosity,

$$d_{f//} = \frac{\frac{4}{3}(\beta^2-1)d_f}{\frac{2\beta^2-1}{\sqrt{\beta^2-1}}\ln(\beta+\sqrt{\beta^2-1}) - \beta} \qquad [5]$$

and

$$d_{f\perp} = \frac{\frac{8}{3}(\beta^2-1)d_f}{\frac{2\beta^2-3}{\sqrt{\beta^2-1}}\ln(\beta+\sqrt{\beta^2-1}) + \beta} \qquad [6]$$

The Stokes number in the models of Harris & Fraser (1976) and Myojo & Takaya (2001) were also based on the Stokes law of a fiber traveling in a tube. The equation for a random orientation fiber was simplified as follows:

$$Stk_i = \frac{\rho d_f^2 U_0 \sin\lambda}{16\mu\left(\frac{0.385}{\ln(2\beta)-0.5} + \frac{1.230}{\ln(2\beta)+0.5}\right) R_0} \qquad [7]$$

where λ is the angle between the initial and final directions of flow at a bifurcation (taken at 30°). In order to simplify the calculation, a fiber equal-volume Stokes number was defined in the model of Zhang et al. (1996) as

$$Stk = \frac{\rho d_{ev}^2 U_0}{36\mu R_0} \qquad [8]$$

where d_{ev}=$d_f\beta^{1/3}$. When summarizing those three Stokes numbers, the following equation was obtained:

$$Stk = \frac{\rho d_f^2 U_0}{36\mu R_0} X_i \qquad [9]$$

where i = 1, 2, or 3 representing the three cases discussed above (1 for Cai & Yu's model, 2 for Harris & Fraser's & Myojo & Takaya's models, and 3 for volume equivalent diameter) and X is a function of β expressed as

$$X_1 = \frac{\beta}{\left(1-\frac{\pi^2}{16}\right)\frac{\frac{4}{3}(\beta^2-1)}{\frac{2\beta^2-1}{\sqrt{\beta^2-1}}\ln(\beta+\sqrt{\beta^2-1})-\beta} + \frac{\pi^2}{16}\frac{\frac{8}{3}(\beta^2-1)}{\frac{2\beta^2-3}{\sqrt{\beta^2-1}}\ln(\beta+\sqrt{\beta^2-1})+\beta}} \qquad [10]$$

$$X_2 = \frac{9\sin\lambda}{4\left(\frac{0.385}{\ln(2\beta)-0.5} + \frac{1.230}{\ln(2\beta)+0.5}\right)} \qquad [11]$$

$$X_3 = \beta^{2/3} \qquad [12]$$

When we compared these three factors as shown in Figure 1, we found that the ratio of X_2 and X_1 is a constant number (0.747 ± 0.005). This indicates that we can easily compare the models of Cai & Yu (1988), Harris & Fraser (1976), and Myojo & Takaya by correcting the Stokes number using the constant ratio. The Stokes number in our experimental data was calculated using the method of Cai & Yu (1988) when compared with these models. The equal-volume Stokes number was used for comparing our model with that of Zhang et al. (1996) to develop our new empirical model.

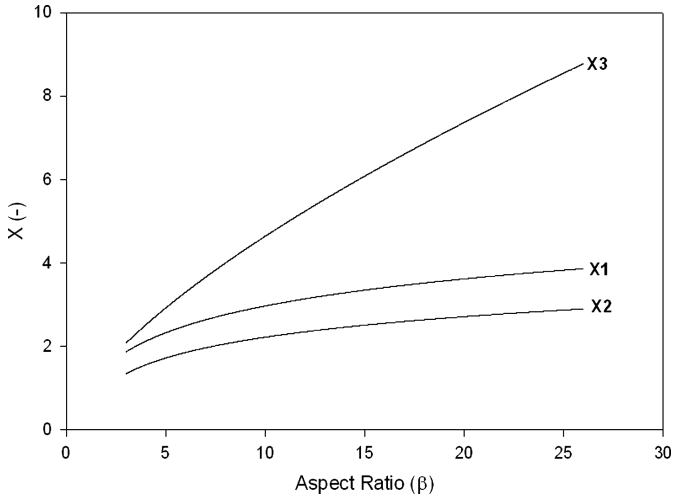

FIG. 1. Comparison of three shape factors as a function of fiber aspect ratio.

RESULTS

Comparison of Experimental Data and Deposition Equations

We compared existing theoretical and empirical models with our experimental data to determine which model could best describe the experimental results.

Figure 2 shows the comparison of our data with three models, Cai & Yu (1988), Harris & Fraser (1976), and Myojo & Takaya (2001), in one of the second bifurcations of our lung cast A. The experimental data were plotted as a function of Stk_1 for random orientation. Stk_2 used by Harris & Fraser (1976) and Myojo & Takaya (2001) was adjusted to Stk_1. Because the models of Cai & Yu (1988) and Harris & Fraser (1976) include bifurcation geometry, the comparison must be made to each individual bifurcation of the cast. Results similar to those of Figure 2 were obtained when we compared the other bifurcations of the two lung casts. There are four empirical equations in the Myojo & Takaya's model (2001), each having different interception parameters. The one shown in Figure 2 was the closest to our experimental data. Figure 2 shows that the models of Cai & Yu, and Harris & Fraser are in good agreement with the experimental data for $Stk_1 > 0.2$, whereas the Myojo & Takaya model overestimated the deposition for $Stk_1 < 0.2$.

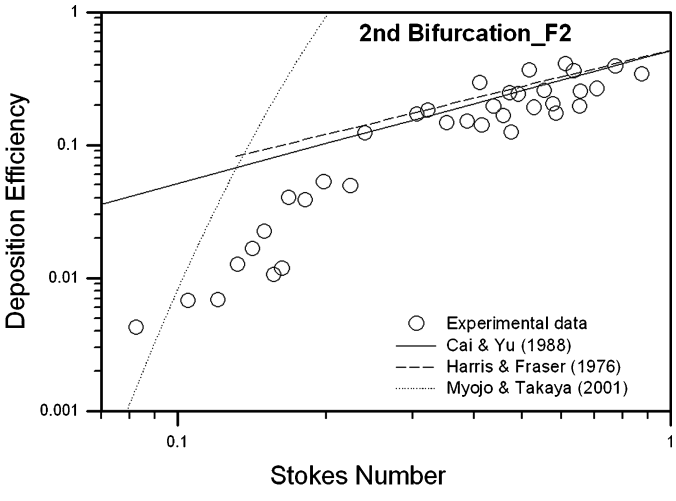

FIG. 2. Experimental data compared with theoretical and empirical models at one bifurcation (F2 in Zhou et al., 2007) of the second generation.

The model of Zhang and co-workers (1996) is difficult to compare as it is not as easy to calculate as the three used in Figure 2. We found it difficult to use because it was based on a CFD method. The other reason we didn't include their model in Figure 2 is due to the different expression of the Stokes number. The Stokes number used in Figure 2 was based on the equivalent diameter of Stokes drag for a fiber with random orientation in the stream as discussed in the previous section. However, the diameter used in the Stokes number by Zhang et al. (1996) was simply a volume equivalent diameter, i.e. the diameter of a sphere that has the same volume as the fiber. In their study, the deposition efficiency was affected by the Stokes number, Reynolds number, and the bifurcation angle. Using their numerical results we obtained a best-fit equation, which is similar to that shown in their study of spherical particles (Zhang et al., 1997), by using the nonlinear curve fitting procedure of SigmaPlot software (SPSS, Chicago, IL) as follows:

$$\eta/\mathrm{Re}^{1/3}\sin\theta = 0.0008\exp(14.49Stk^{0.77}) \quad \text{for } Stk < 0.08$$
$$\eta/\mathrm{Re}^{1/3}\sin\theta = 0.175 - 0.177\exp(-5.55Stk^{1.90}) \quad \text{for } Stk \geq 0.08 \qquad [13]$$

As the formula includes the bifurcation angle and Reynolds number in the Y axis, the comparison can be made for all experimental data regardless of the bifurcation geometry. Figure 3 shows the comparison of our experimental data and the model of Zhang et al. (1996) with the complete set of data from cast A. The data of Sussman et al. (1991a) was also included in this figure as the lung cast experimental data for a small Stokes number range. The comparison indicates that, in general, the experimental data agreed well with Zhang's numerical results over a Stokes number range between 0.001 and 1.0, but the data may not describe results for a specific bifurcation.

The empirical model developed by Sussman and co-workers (1991b) includes many parameters such as fiber size and lung geometry. This model was used to calculate fiber deposition in the bifurcations of our lung cast. Figure 4 shows our experimental data and their calculation for one bifurcation of the second generation of cast A. We also obtained similar results in other bifurcations. Because the model of Sussman et al. (1991b) takes

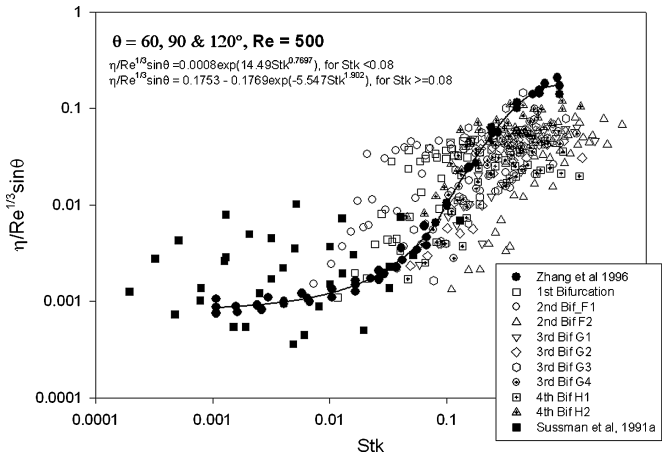

FIG. 3. Comparison of fiber deposition experimental data with the model of Zhang et al. (1996) (solid circles) and data from Sussman et al. (1991a) (solid squares) for all bifurcations of lung cast A. The curve is the regression of Zhang's data.

into account the fiber length, one fiber length generated one curve. In our experiment, there were 12 fiber lengths resulting in 12 equations in each bifurcation. The curves in Figure 4 were boundaries of those 12 equations. The solid lines are the boundaries of the model for flow rate smaller than 30 L/min and the dash lines are boundaries for flow rate larger than or equal to 30 L/min. It appears that the model underestimated deposition when the impaction parameter was larger than 0.001.

Empirical Deposition Equations

From the comparison of models and experimental data described in the previous section, no theoretical or empirical model can be used to describe our fiber deposition data for every bifurcation of the lung casts. In order to predict fiber deposition in human lungs, an empirical model was developed. The derivation of this empirical equation followed the approach we used for the deposition of spherical particles (Zhou & Cheng, 2005). The basic equation considered is the same as we described in Zhou & Cheng (2005),

$$\eta = 1 - \exp(-a \cdot Stk^b) \qquad [14]$$

where a and b are constant numbers for each individual bifurcation or trachea, the Stokes number here is defined in Equation 8.

The experimental data for each bifurcation of casts A and B, which were obtained in our previous study (Zhou et al., 2007), was used to obtain the fitted Equation 14. The result for the constant values of a and b is listed in Table 1. We treated b as a constant value like we did for spherical particles (Zhou & Cheng, 2005). We found that the average value of b (1.34 ± 0.19) is exactly the same as we obtained for spherical particles, although the standard deviation was relatively large. For value a, we plotted the data of F as a function of a (shown in Figure 5) as we did for the spherical particle study (Zhou & Cheng, 2005). An equation of $a = 1.70$ F was obtained, even though the linear relation was not as good as that for spherical particles. Thus, the empirical fiber deposition model for the different bifurcations is expressed as:

$$\eta = 1 - \exp\left(-1.70F\left(\alpha, \frac{R}{R_0}\right) \cdot Stk^{1.34}\right) \qquad [15]$$

As a reference, the equation obtained for spherical particle deposition in a lung cast (Zhou & Cheng, 2005) is also listed here:

$$\eta = 1 - \exp\left(-5.39F\left(\alpha, \frac{R}{R_0}\right) \cdot Stk^{1.34}\right) \quad \textit{for spherical particles} \qquad [16]$$

The trachea is a special region in the respiratory system and it has no bifurcation. Therefore, the geometric factor F is a

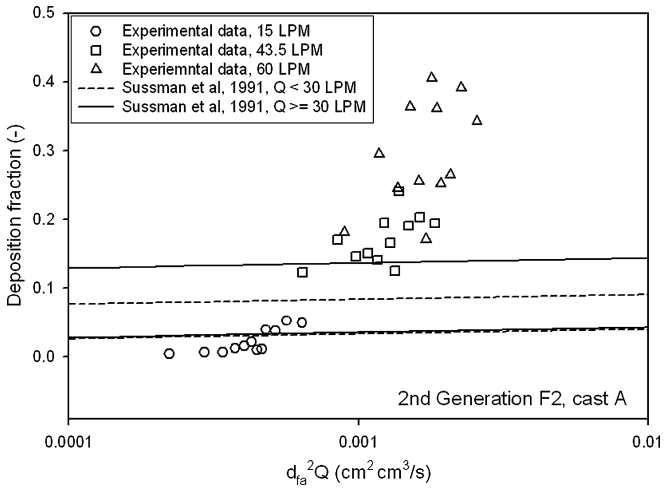

FIG. 4. Comparison of fiber deposition experimental data with the empirical model of Sussman et al. (1991a) in bifurcation F2.

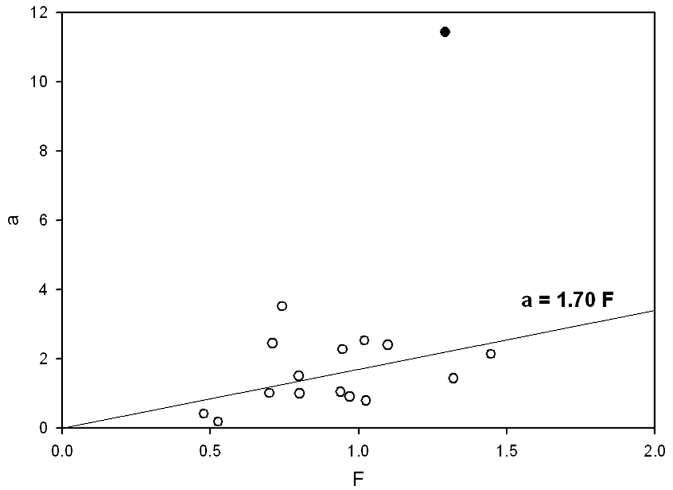

FIG. 5. The constant value a in Equation 14 as a function of F obtained from Equation 16 of Cai & Yu (1988).

TABLE 1
Constant values of a and b obtained by Equation 5 for each bifurcation

	[a]Bifurcation No.	$F(\alpha, R/R_0)$	a	b
Cast A	1_E	0.75	3.51	1.515
	2_F1	1.33	1.43	1.525
	2_F2	0.51	0.19	1.504
	3_G1	0.97	0.91	1.201
	3_G2	0.49	0.41	1.177
	3_G3	0.69	1.01	1.234
	3_G4	0.93	1.05	1.263
	4_H1	1.03	0.79	1.261
	4_H2	1.09	2.41	1.222
Cast B	1_E	0.72	2.45	1.605
	2_F1	0.93	2.27	1.53
	2_F2	0.80	1.00	1.036
	3_G1	1.30	11.44	1.719
	3_G2	0.79	1.51	1.191
	3_G3	1.03	2.53	1.256
	3_G4	1.43	2.13	1.26

[a]Details of the bifurcation number is described in Zhou et al., 2007.

constant at this point. From the regression of the deposition data of casts A and B as shown in Figure 6, the empirical equation for the trachea is:

$$\eta = 1 - \exp(-1.02 \cdot Stk^{0.87}). \quad [17]$$

For spherical particles, the deposition equation in the trachea is:

$$\eta = 1 - \exp(-6.40 \cdot Stk^{1.19}). \quad [18]$$

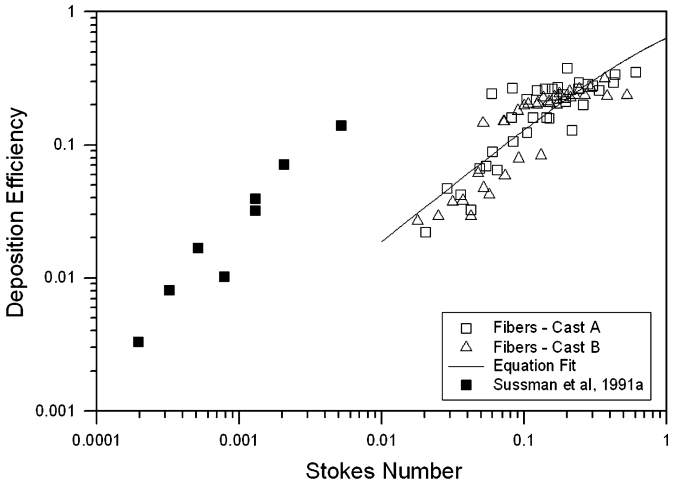

FIG. 6. Equation regression in the tracheal region and compared with data from Sussman et al. (1991a).

DISCUSSION

In general, theoretical models were based on an ideal bifurcation which had the same diameter for each tube and the same geometry of each daughter tube. In a realistic airway tube, the cross-section varied. Also daughter tubes of a bifurcation were not symmetrical in terms of diameter, length and bifurcation angle. Differences between theoretical models and experimental data from a realistic airway cast are expected because of the variation of bifurcation geometry. However, the comparison is still useful to determine if a theoretical model can predict deposition in a realistic airway.

The models of Cai & Yu (1988) and Harris & Fraser (1976) showed good agreement with the experimental data for $Stk_1 > 0.2$, where impaction is the dominant mechanism for fiber deposition. But these theoretical models predicted higher deposition for $Stk < 0.2$. The reasons for these discrepancies are not known. But one reason may be that the theoretical models do not consider the specific characteristic fiber's motion. The empirical models of Myojo & Takaya (2001) and Sussman et al. (1991b) are based on experimental data from fibers with small diameters. It is not surprising to find these models are only valid in the small Stokes number range.

In general, the numerical model of Zhang et al. (1996) follows the general trend of the experimental data for the entire range of the Stokes number used for the available experimental data ($0.001 < Stk < 1.0$). This is because the numerical model considers fiber dynamics as having both translational and rotational motion. It is a good model for calculating the impaction deposition of fibers in tracheobronchial airway generations of symmetrical bifurcation models used in many lung deposition and dosimetry models. However, it may not be accurate in predicting the fiber deposition in a specific airway bifurcation of a realistic and asymmetric airway. Their simulation is based on a single ideal airway bifurcation with uniform diameter of each tube and the same dimensions for daughter tubes. The flow rate splits equally into two daughter tubes. One would not expect that it works for every complicated airway branch with each having a different geometrical parameter.

The empirical model of the current study was based on the experimental data in each bifurcation. Figure 7 shows that our empirical model applies to all generations of cast A, except for one bifurcation for each generation. Even though the fiber deposition data showed a large scatter as a function of the Stokes number, the empirical model covers most of the data. The empirical model can provide a more accurate estimate of fiber deposition in a human tracheobronchial airway bifurcation for a Stokes number >0.001 or in a dominant region of impaction. We are working on fiber deposition experiments using smaller diameter fibers and it will be interesting to determine whether this empirical equation will agree with the additional data.

As discussed in our experimental paper (Zhou et al., 2007), the spherical particle deposition was higher than fiber deposition at a given Stokes number. Figure 8 compares the empirical models of spherical particle deposition (Zhou & Cheng, 2005)

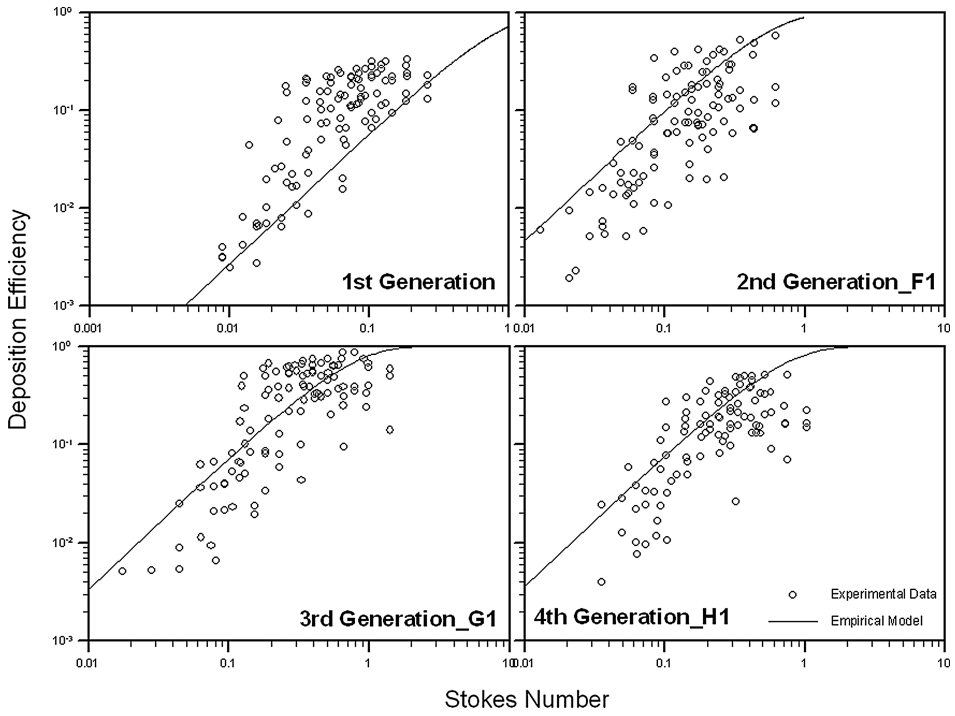

FIG. 7. Comparison of experimental data with the new empirical model in all four generations of cast A. Only one bifurcation is shown for generations two to four.

with that of fiber deposition in our lung casts. A similar trend was also obtained by the theoretical models developed by Zhang et al. (1996, 1997), also shown in Figure 8. This result indicates that fibers can penetrate the upper respiratory airways easier than spherical particles and reach the lower airway. As shown by theoretical simulation (Zhang et al. 1996), this is probably due to the fact that the fiber tends to align itself in the flow. The alignment of the fiber results in small drag in the direction of flow and larger drag in the vertical direction, and therefore lower deposition in the vertical direction. Similarly, we also have

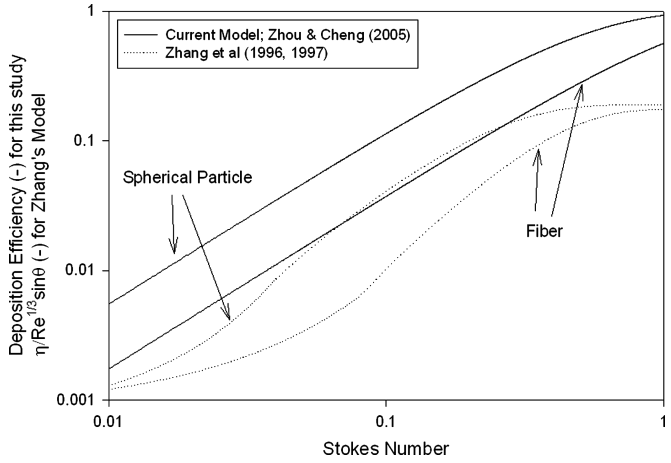

FIG. 8. Comparison of theoretical or empirical models between fibrous and spherical particles.

experimental evidence to show that fibers deposited less than spherical particles of equivalent Stokes number in the human nasal and oral airways (Su & Cheng, 2005, 2006a, 2006b). So far these observations are in the inertial-dominant region. Whether similar observations can be validated for nanofibers where diffusion is the dominant deposition mechanism remains to be seen.

CONCLUSIONS

Extensive comparison of experimental data with existing deposition equations for fiber aerosols in the impaction dominant region shows that existing equations have their limitation. The numerical model of Zhang et al. (1996) follows the general trend of the experimental data for the entire range of the Stokes number used for the available experimental data ($0.001 < Stk < 1.0$). This is because the numerical model considers fiber dynamics as having both translational and rotational motion. Other theoretical models do not consider this particular aspect of fiber dynamics. However even the model of Zhang et al. (1996) could not be expected to yield accurate deposition efficiency in a particular bifurcation. Our new empirical model was developed based on the fiber deposition data from two human lung casts. This model can be used to estimate the fibrous particle inhalation dosimetry and deposition patterns in a specific airway bifurcation. Further, the experimental evidence shows that fibers have lower deposition efficiency as compared with spherical particles of equivalent Stokes number. The numerical model of Zhang et al. (1996) shows that this is probably because the fiber tends to align with

the air flow, and thus can penetrate the head airways and upper tracheobronchial airways.

REFERENCES

Asgharian, B., and Anjilvel, S. 1995. Movement and deposition of fibers in an airway with steady viscous flow. *Aerosol Sci. & Technol*. 22:261–270.

Asgharian, B., and Yu, C. P. 1988. Deposition of inhaled fibrous particles in the human lung. *J. Aerosol Med.* 1:37–50.

Asgharian, B., and Anjilvel, S. 1998. A multiple-path model of fiber deposition in the rat lung. *Toxicol. Sci.* 44(1):80–86.

Balásházy, I., Moustafa, M., Hofmann, W., Azoke, R., El-Hussein, A., and Ahmed, A. 2005. Simulation of fiber deposition in bronchial airways. *Inhal. Toxicol.* 17:717–727.

Beeckmans, J. M. 1970. The deposition of asbestos particles in the human respiratory tract. *Int. J. Environ. Studies* 1:31–34.

Cai, F. S., and Yu, C. P. 1988. Inertial and interceptional deposition of spherical particles and fibers in a bifurcating airway. *J. Aerosol Sci*. 19:679–688.

Ding, J. Y., Yu, C. P., Zhang, L., and Chen, Y. K. 1997. Deposition modeling of fibrous particles in rats: comparisons with available experimental data. *Aerosol Sci. Technol.* 26:403–414.

Evans, J. C., Evans, R. J., Holmes, A., Hounam, R. F., Jones, D. M., Morgan, A., and Walsh, M. 1973. Studies on the deposition of inhaled fibrous material in the respiratory tract of rat and its subsequent clearance using radioactive trace techniques (I. UICC crocidolite asbestos). *Environ. Res*. 6:180–201.

Griffis, L. C., Henderson, T. R., and Pickrell, J. A. 1981. A method for determining glass in rat lung after exposure to a glass fiber aerosol. *Am. Ind. Hygiene Assoc. J*. 42:566–569.

Harris, R. L. 1972. A model for deposition of microscopic fibers in the human respiratory system. *Doctoral thesis*. University of North Carolina, Chapel Hill.

Harris, R. L., and Fraser, D.A. 1976. A model for deposition of fibers in the human respiratory system. *Am. Ind. Hygiene Assoc. J.* 37:73–89.

Morgan, A., Talbot, R. J., and Holmes, A. 1978. Significance of fiber length in the clearance of asbestos fibers from the lung. *Brit. J. Ind. Med*. 35:146–153.

Myojo, T. 1987. Deposition of fibrous aerosol in model bifurcating tubes. *J. Aerosol Sci.* 18:337–347.

Myojo, T. 1990. The effect of length and diameter on the deposition of fibrous aerosol in a model lung bifurcation. *J. Aerosol Sci.* 21:651–659.

Myojo, T., and Takaya, M. 2001. Estimation of fibrous aerosol deposition in upper bronchi based on experimental data with model bifurcation. *Ind. Health*. 39:141–149.

Oseen, C. W. 1927. *Neuere Methoden und Ergebnisse in der Hydrodynamik*. Akademische Verlagsgesellschaft. Leipzig, p. 18.

Podgorski, A., Gradon, L., and Grzybowski, K. 1995. Theoretical study on deposition of flexible and stiff fibrous aerosol particles in a cylindrical collector. *Chem. Eng. Sci*. 58:109–121.

Roggli, V. L., and Brody, A. R. 1984. Changes in numbers and dimensions of chrysotile asbestos fibers in lungs of rats following short-term exposure. *Exp. Lung Res*. 7:133–147.

Sturm, R., and Hofmann, W. 2006. A computer program for the simulation of fiber deposition in the human respiratory tract. *Comput. Biol. Med*. 36:1252–1267.

Su, W. C., and Cheng, Y. S. 2005. Deposition of fiber in the human nasal airway. *Aerosol Sci. Technol.* 39:888–901.

Su, W. C., and Cheng, Y. S. 2006a. Fiber deposition in two human respiratory tract replicas. *Inhal. Toxicol.* 18:749–760.

Su, W. C., and Cheng, Y. S. 2006b. Deposition of fiber in a human airway replica. *J. Aerosol Sci.* 37:1429–1441.

Sussman, R. G., Cohen, B. S., and Lippmann, M. 1991a. Asbestos fiber deposition in human tracheobronchial cast. I. Experimental. *Inhal. Toxicol.* 3:145–160.

Sussman, R. G., Cohen, B. S., and Lippmann, M. 1991b. Asbestos fiber deposition in human tracheobronchial cast. II. Empirical model. *Inhal. Toxicol.* 3:161–178.

Task Group on Lung Dynamics. 1966. Deposition and retention models for internal dosimetry of the human respiratory tract. *Health Phys*. 12:173–207.

Weibel, E. R. 1963. *Morphometry of the Human Lung*. New York: Academic Press.

Zhang, L., Asgharian, B., and Anjilvel, S. 1996. Inertial and interceptional deposition of fibers in a bifurcation airway. *J. Aerosol Med.* 9:419–430.

Zhang, L., Asgharian, B., and Anjilvel, S. 1997. Inertial deposition of particles in the human upper airway bifurcations. *Aerosol Sci. Technol.* 26:97–110.

Zhou, Y., and Cheng, Y. C. 2005. Particle deposition in a cast of human tracheobronchial airways. *Aerosol Sci. Technol.* 39:492–500.

Zhou, Y., Su, W. C., and Cheng, Y. C. 2007. Fiber deposition in the tracheobronchial region: Experimental measurements. *Inhal. Toxicol.* 19:1071–1078.